JOURNAL OF CATALYSIS 117, 102–120 (1989)

A Controlled Atmosphere *in Situ* X-Ray Diffraction Study of the Activation and Performance of Ammonia Synthesis Catalysts Derived from $CeRu_2$, $CeCo_2$, and $CeFe_2$

ANDREW P. WALKER, TREVOR RAYMENT, AND RICHARD M. LAMBERT[1]

Department of Chemistry, University of Cambridge, Lensfield Road, Cambridge CB2 1EP, England

Received June 29, 1988; revised November 17, 1988

Highly active ammonia synthesis catalysts derived from cerium intermetallic alloy precursors $CeRu_2$, $CeCo_2$, and $CeFe_2$ have been studied by *in situ* powder X-ray diffraction (XRD) with concurrent analysis of catalytic activity. The reaction was investigated at pressures of up to 50 bar and at temperatures up to 550°C. Precursor activation was carried out in pure hydrogen, N_2/H_2, and CO/H_2 under various regimes of temperature and pressure. It is found that the formation of active catalysts depends upon the presence of cerium hydride and transition metal crystallites in the ultimate material, although there is no correlation between XRD-derived metal areas and chemical rates. The corresponding transition metal/cerium dioxide catalysts have a much lower activity for ammonia synthesis. The special activity of the hydride-based catalysts may arise from an intimate interaction between the support phase and the ultradispersed transition metal particles.

INTRODUCTION

Catalysts derived from rare earth intermetallic precursors can exhibit very high specific activities for ammonia synthesis; in some cases the reported performance exceeds that of the well-established Fe-based industrial catalyst by as much as an order of magnitude (*1*). Discharged catalysts of this type have been examined by XRD methods (*1, 2*), although such measurements are of limited value due to the extreme air sensitivity of these materials. In this paper we report on the results of a controlled atmosphere XRD study of the genesis and reactive behavior of ammonia synthesis catalysts derived from $CeRu_2$, $CeCo_2$, and $CeFe_2$; these observations were coupled with concurrent measurements of the catalytic activity. The power of this combination of techniques has already been demonstrated by our earlier work on methanol synthesis catalysts derived from Cu/rare earth intermetallics (*3*). In the present case a comparison is made between hydride-based catalysts and the corresponding oxide-based materials. Significantly, it is found that the latter materials are inert ammonia catalysts despite the fact that their Cu analogs are exceedingly active for methanol synthesis (*3*). Furthermore, the observed order of ammonia activities for the hydride-based catalysts is Ru > Co > Fe in contrast to that which characterizes the unpromoted metals themselves (Fe > Ru ≫ Co).

EXPERIMENTAL

The controlled atmosphere cell used for *in situ* XRD measurements has been described in detail elsewhere (*3*). This device was used to investigate the structure and reactivity of alloy specimens at pressures up to 70 bar and temperatures up to 550°C. Most of the XRD data were collected using conventional Bragg–Brentano reflection geometry. This method offers optimum intensities but the effective penetration depth into the sample bed is only 1–2 μm for the materials used in this study. Since the granule size was 50–250 μm, core/shell effects could have escaped detection. Some addi-

[1] To whom correspondence should be addressed.

0021-9517/89 $3.00

tional measurements were therefore made in transmission geometry, in which arrangement the beam penetrates the whole sample. In such experiments the results are truly representative of the bulk material, but counting statistics are poorer because monochromated radiation must be used. In the present case it was found that measurements in transmission and reflection gave the same results, so that core/shell effects can be discounted in this work.

Intermetallic samples were prepared by electron beam melting of the constituent metals under high vacuum followed by annealing at 500°C for 1 month in an evacuated quartz ampoule. For each run an accurately weighed catalyst charge of 0.10–0.20 g was crushed to a particle size of 50–250 μm and loaded into the sample cell under an argon atmosphere; the level of oxygen in the glovebox was never greater than 20 ppm. The cell was then sealed and transferred to the diffractometer. All samples of starting material derived from the three compounds were examined by XRD and found to consist of a single metallic phase. This method of specimen handling also resulted in no detectable oxidation of the fresh precursors.

Reactant gases were obtained from BOC Ltd. (Special Gases) and used without additional purification: hydrogen (CP grade, 99.999% pure), premixed $CO:H_2$ (33:67, impurities O_2 5 ppm, H_2O 2 ppm, and CO_2 20 ppm), and premixed $N_2:H_2$ (25:75, impurities O_2 4 ppm and H_2O 4 ppm). For some of the work a premixed 25:75 $N_2:H_2$ gas mixture was obtained from Cryoservices Ltd. and, again, was used without further purification (O_2 4 ppm and H_2O 2 ppm). Flow rates of between 15 and 30 standard cubic centimeters per minute (sccm) were used with total gas pressures of between 5 and 50 bar. Production of ammonia was monitored by measuring the intensity of the infrared absorbance of NH_3 ($\tilde{\nu} \sim 3320\ cm^{-1}$) in the effluent stream using a Perkin–Elmer 599 IR spectrometer programmed to record spectra at specified time intervals. Detection sensitivity was enhanced by use of a gas cell with 6-mm quartz windows which permitted sampling at 5 bar (detection limit 200 ppm ammonia).

Quantitative analysis of the XRD data was performed by fitting Cauchy, pseudo-Voigt, and, in some cases, split Pearson functions to the observed peak profiles in order to obtain peak widths (FWHM) and integrated peak intensities. Particle sizes were obtained from the diffraction profiles via the Scherrer equation after making allowance for instrumental broadening. The application of more sophisticated methods (e.g., Warren–Averbach) was hampered by considerable overlap of the diffraction lines for the cerium- and transition-metal-containing phases, except for the lowest order of reflection. Hence only single-line methods are applicable, and these indicated a considerable spread of particle sizes in all samples, centered around the value given by the Scherrer equation. The Scherrer equation has been used in preference throughout the work since

(a) considerable differences in particle size exist between the catalysts derived from the three kinds of alloy;

(b) within any system and for a given experiment the *changes* in peak shape provide greater insight than the absolute particle size values.

RESULTS

The intermetallic alloys $CeRu_2$, $CeCo_2$, and $CeFe_2$ all possess the $MgCu_2$ (C 15 type) structure (*4–6*). Experiments were carried out over a range of conditions to characterize the structural and chemical behavior of these alloy precursors, and the catalysts derived from them. Particular attention was given to following the evolution of the various solid phases and to the conditions required for onset of ammonia synthesis activity. The effects of temperature on particle growth and the consequences of using a variety of different activation procedures have also been investigated. In particular, the effects of activating the alloy

precursors in H_2, $N_2 + H_2$, and $CO + H_2$ are described below.

$CeRu_2$ Precursors

a. Interaction of $CeRu_2$ with H_2. The diffraction patterns illustrated in Fig. 1 show that short-term (~1-hr) exposure of this alloy to 20 bar of hydrogen at room temperature resulted in gradual loss of diffraction lines due to the starting material, with concurrent appearance and growth of new peaks. This new phase is an intermetallic hydride, $CeRu_2H_x$, where x lies between 4 (*7*) and 5 (*8, 9*). The XRD data show that the cubic Laves phase structure of the original intermetallic is preserved upon hydrogenation, although significant lattice expansion occurs; the lattice parameter of the intermetallic hydride is ~8.4 Å, which agrees well with previous observations (*8, 9*).

Figure 1 also shows that continued exposure (~4 hr) to hydrogen under the same conditions of temperature and pressure led to the emergence of another phase, which is almost certainly a second intermetallic hydride since metallic Ru features are completely absent from the diffraction patterns. It has not yet been possible to assign a structure to this second intermetallic hydride phase. These two intermetallic (ternary) hydrides coexist over a broad range of temperature and pressure. Figure 2 shows that both phases were stable under 40 bar of hydrogen at 200°C; raising the temperature to 250°C resulted in the gradual loss of both ternary hydrides. Increasing the temperature to 300°C caused further decomposition of both hydrides, and the appearance of an intense broad peak centered on $2\theta \sim 28°$. However, both intermetallic hydride phases, once formed at low temperature, exhibited significant stability (~1 hr) upon raising the temperature directly to 450°C.

The effect of raising the temperature of

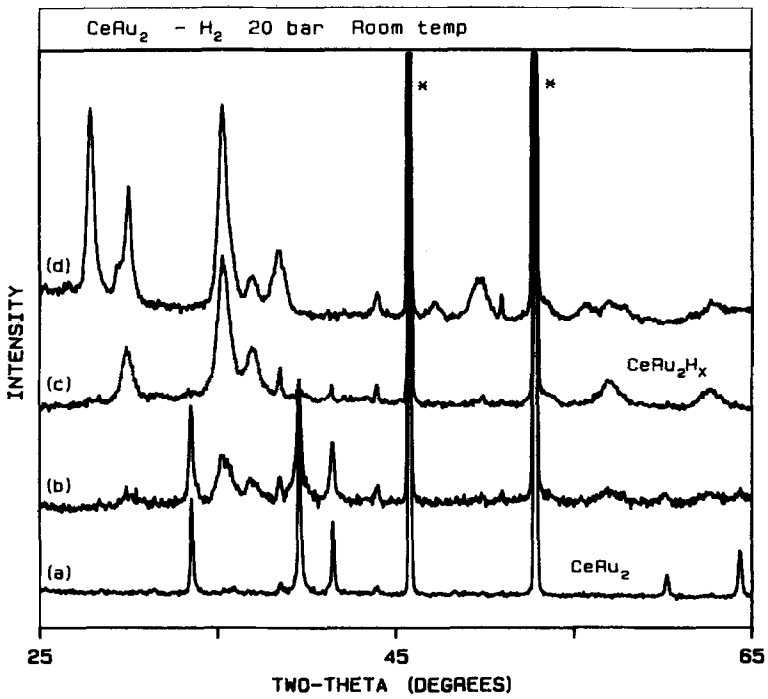

FIG. 1. Room temperature hydrogen activation of the $CeRu_2$ precursor alloy. Exposure time (a) 0 hr, (b) 1 hr, (c) 2 hr, (d) 4 hr. (*Peaks due to the sample holder.)

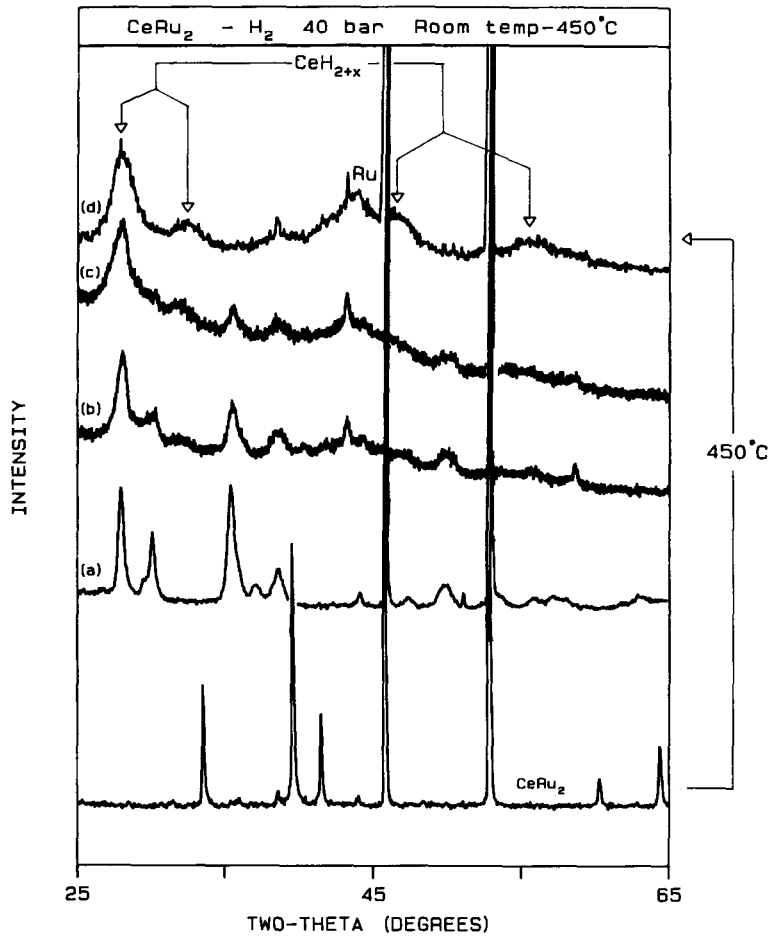

FIG. 2. Hydrogen activation of $CeRu_2$ at increasing temperature. (a) After 2 hr at 200°C, (b) 250°C, (c) 300°C, (d) 450°C.

the precursor directly to 450°C in 40 bar of hydrogen is also illustrated in Fig. 2. Under these conditions no intermetallic hydride peaks appeared in the diffraction patterns; instead, the original alloy was rapidly converted to an fcc structure with lattice parameter characteristic of the nonstoichiometric *binary cerium hydride,* CeH_{2+x} ($0 \leq x \leq 1$). The binary rare earth hydrides are known to exhibit nonstoichiometry over a wide range of composition without undergoing any change in structural type. In the case of cerium hydride, the fluorite structure is preserved from $CeH_{1.8}$ to CeH_3 (*10*). In addition, Fig. 2 also reveals that decomposition of the intermetallic (ternary) hydrides *also* results in formation of this binary cerium hydride. That is, there appear to be two routes for hydrogenolysis of the alloy, one of which does not involve transient formation of the intermetallic hydride.

Heating the starting alloy to $\gtrsim$250°C in hydrogen (Fig. 2) also led to the appearance of a broad peak centered around 44–45°; this is due to the presence of crystallites of ruthenium metal. The peak showed a gradual increase in intensity over a 10-hr period at 250°C; at higher temperatures it grew more rapidly, while still retaining its broad profile. This behavior indicates a rise in the number of Ru crystallites contributing to

the diffraction peak, without significant particle growth; under these conditions, raising the temperature leads to faster expulsion of ruthenium metal. Although analysis of the Ru peak is complicated by its overlap with one of the CeH_{2+x} peaks, the results indicate that the Ru crystallites have a diameter of ~35 Å. The metal particle size increased slightly with time, but even prolonged heating at 550°C did not result in the formation of significantly larger Ru particles. This slow increase in crystallite size was also observed for the CeH_{2+x} phase, where the Debye–Scherrer particle size rose from 55 to 60 Å over a 4-hr period at 450°C. Crystallite growth stopped at this point, and holding the temperature at 550°C for 6 hr did not lead to any further growth. The rise and leveling off of the Ru peak intensity closely parallels that of the CeH_{2+x} peak at $2\theta \sim 28°$, an observation discussed in more detail below.

b. Interaction of $CeRu_2$ with N_2/H_2. The behavior of $CeRu_2$ in the 1:3 $N_2:H_2$ mixture was very similar to that observed in pure hydrogen. Intermetallic hydrides formed under the same conditions of temperature and *total* pressure as in the case of treatment in H_2 alone. In view of this, it would appear that under these conditions, temperature is the critical variable which determines the stability of the intermediate hydrides. Indeed, further experiments showed that the temperature range of intermetallic hydride stability was independent of hydrogen pressure for partial pressures between 5 and 50 bar, both ternary hydrides decomposing to the binary rare earth hydride after 4 hr at 300°C. Raising the temperature to 400°C in the presence of N_2/H_2 resulted in the immediate appearance of diffraction features characteristic of CeH_{2+x} and Ru metal; that is, formation of the ternary hydride phases was not detectable. The broad nature of the Ru peak is clearly apparent and, once more, the intensity of this peak increased with time while the FWHM remained approximately the same. Profile analysis yields initial particle diameters of ~35 Å for Ru and ~60 Å for CeH_{2+x}, close to the values observed under similar conditions in pure hydrogen. At 450°C the Ru particle size increased slowly for the first 5 hr, but then remained constant at ~40 Å; subsequently raising the temperature to 550°C for 6 hr resulted in no further increase in crystallite size.

Ammonia synthesis activity of the CeH_{2+x}/Ru system was monitored at 450°C in 50 bar N_2/H_2. Due to the rapidity with which Ru was expelled from the precursor phase at 450°C (and, indeed, at any temperature high enough to produce a measurable ammonia yield) it was not generally possible to test for correlation between the rise in ammonia yield and the intensity of the transition metal peak. (This was also the case for the Co- and Fe-containing alloys.) However, one $CeRu_2$ sample (and one $CeFe_2$ sample) underwent much slower activation, so that in this case it was possible to follow the time evolution of solid phases and its correlation with catalytic performance. This $CeRu_2$ precursor was pretreated at 100°C in the N_2/H_2 mixture to form the two characteristic intermetallic hydrides. During this treatment, no ammonia activity was detected. On increasing the temperature to 450°C, the ammonia yield rose slowly with time, while the diffraction patterns revealed that the intermetallic hydride phases were still present after 12 hr under these conditions. However, features due to both CeH_{2+x} and metallic Ru appeared after a short interval, and these showed a continued increase in intensity with time. Figure 3 shows that there is a good correlation between the rise and leveling-off of ammonia activity, and the growth of both the transition metal *and* rare earth hydride particles. The ammonia yield leveled off at exactly the value observed for all the other CeH_{2+x}/Ru catalysts. During the course of the reaction the size of the Ru crystallites showed a small but significant increase in size, from ~35 to ~40 Å, indicating that for this sample the ammonia activity did *not* correlate with exposed sur-

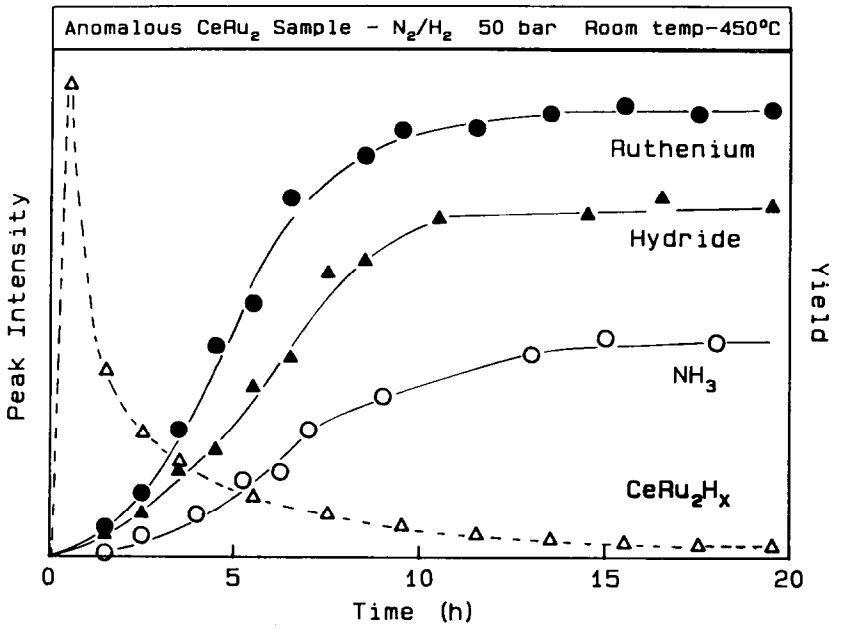

FIG. 3. Structural and activity data for N_2/H_2 activation of the anomalous $CeRu_2$ sample at 50 bar/450°C showing the correlation between the rise of ammonia activity and the growth of the ruthenium and cerium hydride peak intensities.

face area of the Ru crystallites. With every other sample pretreated in this way peaks characteristic of the ternary hydrides exhibited a rapid decrease in intensity on raising the temperature to 450°C and disappeared completely after approximately 1 hr on stream.

No decrease in the activity of *any* of the CeH_{2+x}/Ru catalysts (nor of the Co- or Fe-containing catalysts) was observed over a 48-hr period at 450°C.

Figure 4 shows the variation in ammonia activity of a typical catalyst induced by raising the temperature in a series of steps from 450 through 475°C and 500 to 550°C and finally reducing it back to 450°C. During this treatment the size of the Ru crystallites increased from ~35 to ~40 Å, *but the catalyst showed exactly the same activity during the second period at 450°C as during the first.*

The extreme air sensitivity of the CeH_{2+x}/Ru catalyst was demonstrated by the observation that exposing an activated catalyst to air at room temperature for 1 hr resulted in the complete loss of all activity. XRD analysis revealed that this treatment caused conversion of the hydride to the binary rare earth oxide, CeO_2.

c. Interaction of $CeRu_2$ with CO/H_2. Rare earth/Cu alloys activated in CO/H_2 yield exceedingly active methanol synthesis catalysts which appear to contain an ultradispersed form of Cu (*3*). Accordingly, the effects of such activation procedures were investigated in the present case. The alloy remained unchanged on heating to 200°C in the presence of 40 bar of 1:2 $CO:H_2$ mixture. However, raising the temperature to 300°C resulted in rapid conversion to cerium dioxide and metallic ruthenium. As Fig. 5 shows, a further increase in temperature to 400°C caused the integrated intensities of these diffraction features to rise; this was accompanied by a slight decrease in the FWHM values. The Ru crystallites were again very small (~40 Å); the CeO_2 particle size was larger (~75 Å) than

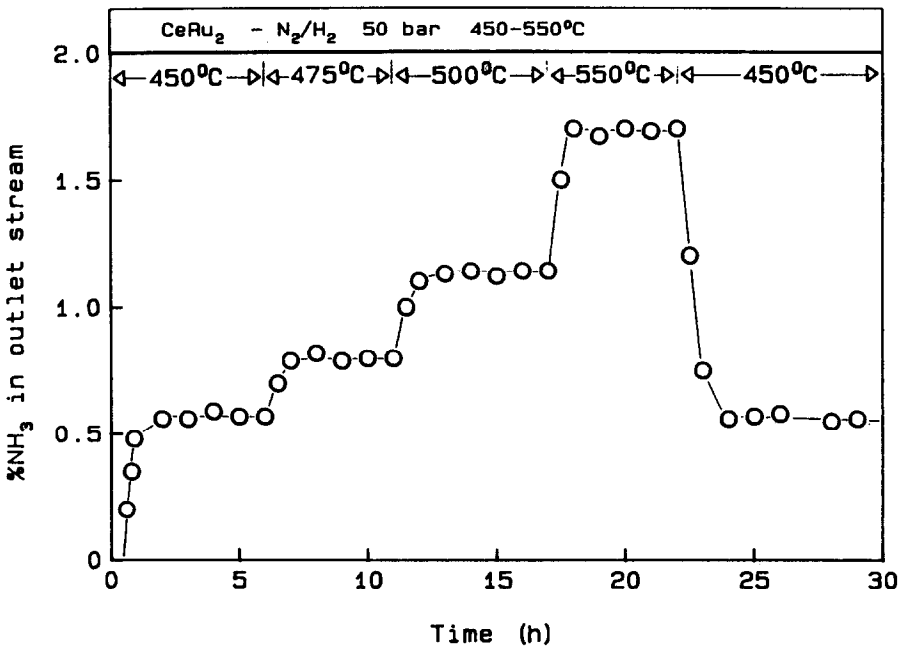

FIG. 4. The effect of increasing the temperature in steps from 450 to 550°C. The activity of the catalyst returns to its original value on reduction of the temperature back to 450°C.

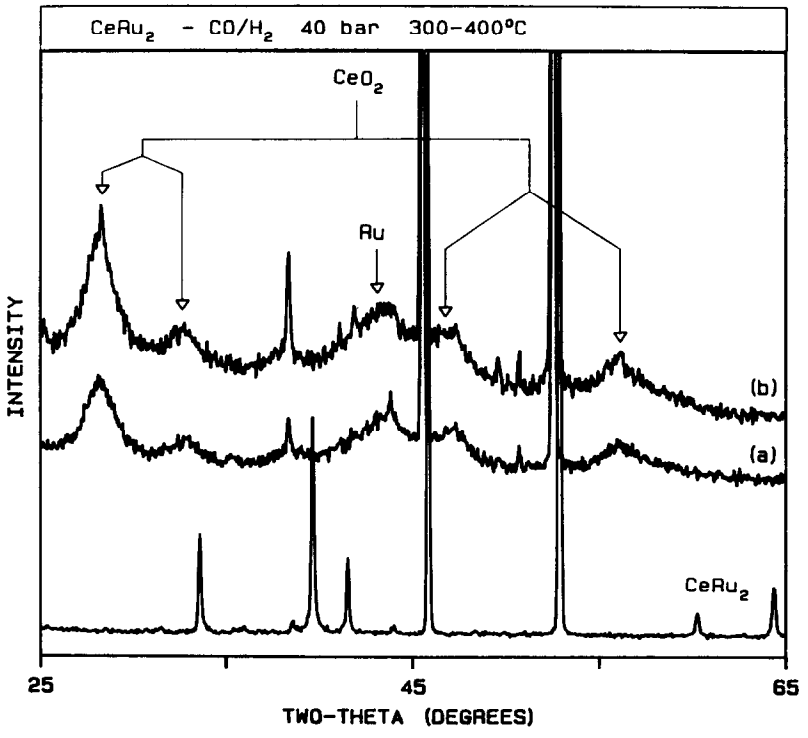

FIG. 5. High-temperature CO/H_2 activation of $CeRu_2$. (a) 300°C; (b) 400°C.

that observed for the CeH_{2+x} crystallites. Maintaining the temperature at 550°C in CO/H_2 did not lead to substantial particle growth of either the rare earth oxide or the ruthenium metal.

Alloys treated in CO/H_2 at temperatures ranging from 300 to 550°C and subsequently exposed to the N_2/H_2 mixture at 450°C showed *no ammonia synthesis activity*. No activity was observed even after 24 hr under 50 bar of N_2/H_2 at 450°C. Increasing the temperature to 550°C eventually led (after 4 hr) to the onset of ammonia synthesis activity. However, the maximum steady-state activity of this oxide-based catalyst was only about one-tenth of that observed for the CeH_{2+x}/Ru system at the same temperature; cooling to 450°C caused the activity to fall back to an undetectable level. It should be noted that CeO_2 was stable under these highly reducing conditions, no conversion to the sesquioxide Ce_2O_3 being observed. This agrees with previous reports (*11, 12*) according to which temperatures exceeding 1000°C are necessary to effect complete reduction to Ce_2O_3.

Nix *et al.* (*3*) reported that prehydriding rare earth/Cu alloys in H_2 before activation in CO/H_2 could lead to higher initial methanol activity in the resulting catalyst; it was also found that the transient formation of intermetallic hydride phases played a critical role in the production of these particular, highly active catalysts. In the present instance, this was *not* found to be the case for ammonia synthesis catalysts. Prehydrogenating to generate the ternary intermetallic hydride phase before switching the gas feed to CO/H_2 to form CeO_2, followed by exposure to N_2/H_2, gave exactly the same low ammonia activity as observed without the intermediacy of the ternary hydrides.

The effect of forming the *binary* rare earth hydride prior to activation in CO/H_2 was also studied. XRD revealed a gradual conversion of hydride to oxide over 3 hr immediately following the switch to CO/H_2. Samples treated in this way followed the same activity pattern for ammonia synthesis as that exhibited by other CeO_2/Ru systems prepared via different routes, i.e., no observable activity at 450°C in 50 bar N_2/H_2, and a small but detectable ammonia yield at 550°C.

One possible explanation for the severely reduced activity of the catalysts activated in CO/H_2 is blockage of active surface sites by carbon. Ru is known to be a very active methanation catalyst and this reaction proceeds with finite probability of carbon deposition when $H_2/CO \leq 2.7$ (*13*) (this work, $H_2/CO = 2$). GC analysis of the effluent gas was therefore used to test this hypothesis, replacing the infrared detection system described earlier. $CeRu_2$ samples activated in 20 bar of CO/H_2 at 450°C did in fact show high methanation activity. After 10 min under these conditions, when XRD indicated that complete conversion to CeO_2 and Ru had taken place, the gas feed was switched to pure hydrogen and CH_4 production was monitored. Peaks due to higher mass hydrocarbons ($\geq C_2$) disappeared shortly after switching, while that due to methane died away over a 10-min period, as did the peak due to water. This indicates that both carbon- and oxygen-containing species remained on the catalyst surface for some time, even when no CO was present in the gas feed and that some, if not all, of these species were removed by flowing hydrogen over the catalyst at 450°C. Experiments in which the CO/H_2 gas feed was followed by a N_2/H_2 mixture gave very similar results.

In these experiments, the time taken for the methane signal to die away increased with initial exposure to the activating CO/H_2 mixture. After a 1-hr activation in CO/H_2 at 450°C, the CH_4 signal disappeared completely after 20 min; after 6 hr exposure to CO/H_2 the CH_4 peak died away over 30 min. It therefore appears that some carbon deposition does indeed occur during activation in CO/H_2 and that the amount of such deposition can be minimized by limiting the exposure to the CO/H_2 mixture. It also seems likely that these species are almost entirely removed over a short period of

time in the N_2/H_2 mixture at 450°C: there was no perceptible difference in ammonia activity at 550°C for samples activated in CO/H_2 for 10 min and those activated for 6 hr under the same conditions. Similar experiments were conducted on samples of $CeCo_2$ and $CeFe_2$ and in both cases the trends were exactly the same as those reported above for the $CeRu_2$-derived catalysts. These results strongly suggest that the very low ammonia synthesis activity of catalysts activated in CO/H_2 is *not* due to extensive carbon deposits which are stable in N_2/H_2. In order to confirm this view, an alternative oxidative activation procedure was used. Oxygen itself could not be employed due to limitations imposed by the beryllium pressure vessel. Instead, a stream of nitrogen containing 100 vpm of water was passed over the starting alloy at 20 bar and 450°C to effect the conversion to the oxide. For each alloy, the ammonia activity over the resulting CeO_2/transition metal system *was the same as previously observed over catalysts preactivated in the CO/H_2 mixture.*

Nix *et al.* (*3*) concluded that the very high methanol activity exhibited by Nd–Cu alloys was attributable to the presence of very small Cu entities invisible to XRD. Therefore a quantitative analysis was made of the amount of expelled Ru visible by XRD. Powdered CeO_2 and powdered Ru were mixed mechanically to produce an intimate mixture with molar ratio 1 : 2 (Ce : Ru). Comparisons of the integrated intensities for this mixture and the CO/H_2 activated catalysts indicated that at least 80% of the Ru present in the starting material was visible as metallic Ru in the diffraction patterns of the activated catalysts.

$CeCo_2$ Precursors

a. Interaction of $CeCo_2$ with H_2. $CeCo_2$ did not react with 40 bar of hydrogen at 175°C, but, as Fig. 6 shows, raising the temperature to 200°C resulted in the formation of an amorphous phase inferred from the

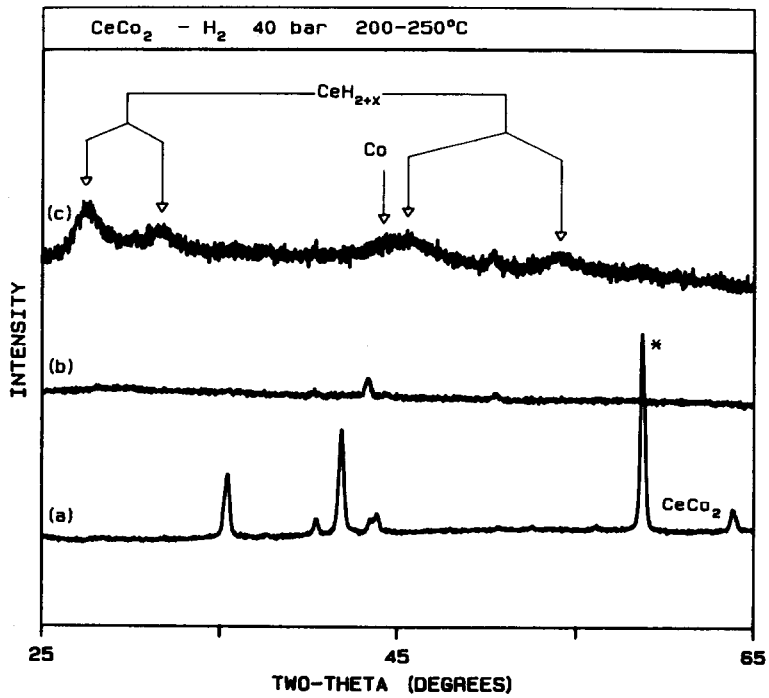

FIG. 6. Hydrogen activation of the $CeCo_2$ precursor alloy. (a) Starting alloy; (b) 200°C, amorphous phase; (c) 250°C.

absence of diffraction peaks other than those due to the cell. This phase had a very limited range of stability, heating to 250°C yielding diffraction features characteristic of CeH_{2+x} and cobalt crystallites. These features showed a gradual intensity rise over a 10-hr period at 250°C, and a more rapid increase at higher temperatures. XRD indicated that raising the temperature directly to 400°C at hydrogen pressures between 5 and 50 bar gave CeH_{2+x} and Co particles only. However, the simultaneous presence of the amorphous phase under these conditions cannot be ruled out. At this temperature the CeH_{2+x} crystallites exhibited an increase in size from 50 to 60 Å over a 4-hr period; i.e., these CeH_{2+x} crystallites have approximately the same diameter as those formed by the $CeRu_2$ system. However, the Co crystallites are larger than the Ru crystallites described earlier, having diameters of ~100 Å.

b. Interaction of $CeCo_2$ with N_2/H_2. The behavior of $CeCo_2$ precursors in N_2/H_2 broadly resembled that observed in pure hydrogen. Low-temperature (200°C) activation again gave the amorphous phase, which converted to CeH_{2+x} and Co on heating to 250°C or above; the Co crystallites again had diameters of ~100 Å. However, in contrast to the observations made in pure hydrogen, holding the temperature at 450°C in 50 bar of N_2/H_2 for several hours resulted in the series of diffraction patterns shown in Fig. 7. A shoulder appeared on the CeH_{2+x} peak at $2\theta \sim 31°$ and increased in intensity over a 4-hr period, beyond which it remained constant. This feature may be assigned to cerium nitride, CeN; the activity of the catalyst did not correlate with the integrated intensity of the CeN peak. The CeH_{2+x}/Co system was less active for ammonia synthesis than CeH_{2+x}/Ru at all temperatures between 450 and 550°C as shown in Table 1. As with CeH_{2+x}/Ru, increasing the temperature from 450 to 550°C led to a

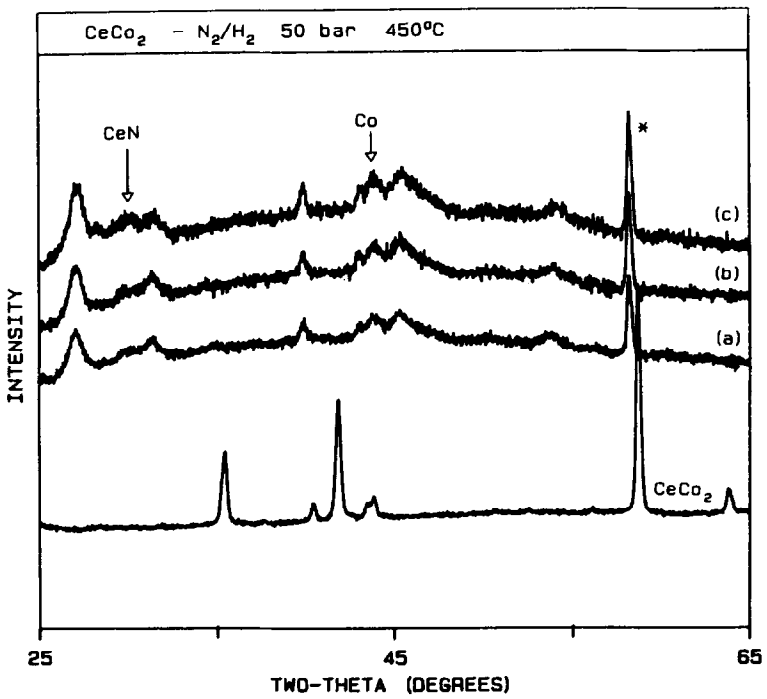

FIG. 7. N_2/H_2 activation of $CeCo_2$ at 50 bar/450°C showing the gradual growth of the CeN peak. (a) After 1 hr, (b) 2 hr, (c) 4 hr.

TABLE 1

Activities of the Three Systems at 50 Bar in a 1 : 3 N_2 : H_2 Mixture

Catalyst system	Temperature (°C)	Activity $\times 10^5$ (mol NH_3/g cat^{-1} min^{-1})
CeH_{2+x}/Ru	450	4.55
	500	9.17
	550	13.80
CeH_{2+x}/Co	450	3.25
	500	4.95
	550	6.90
CeH_{2+x}/Fe	450	2.60
	500	3.81
	550	5.60

rise in activity, the reaction rate falling back to its original value on cooling to 450°C, despite the small but significant Co crystallite growth (from ~100 to ~108 Å) which occurred over the period at 550°C.

c. Interaction of $CeCo_2$ with CO/H_2. Treatment of the alloy with 40 bar of CO/H_2 at temperatures ≥250°C led to the formation of CeO_2 and cobalt crystallites. The Co particles had diameters of ~115 Å and showed little change in size even after prolonged heating at 550°C; i.e., as with the Ru-containing alloy, the transition metal particles were larger when produced in the oxide matrix. The CeO_2 particles were ~75 Å in diameter, approximately the same size as observed with $CeRu_2$-derived catalysts. No ammonia activity was observed from the CeO_2/Co system in 50 bar of N_2/H_2 at temperatures between 450 and 550°C. Furthermore, in contrast to the behavior of the CeH_{2+x}/Co catalyst, no peak due to CeN appeared in the diffraction patterns on switching the gas feed from CO/H_2 to N_2/H_2. In addition, once CeN had been formed by activation in the N_2/H_2 mixture, even extended exposure to CO/H_2 did not lead to a reduction in the intensity of the nitride peak. These two observations indicate that no nitride/oxide interconversion took place under these conditions. Exactly the same observations (both in terms of the phases present and in terms of the catalytic activity) were made when preactivating $CeCo_2$ to form *either* the intermetallic hydride *or* the binary rare earth hydride en route to the oxide.

$CeFe_2$ Precursors

a. Interaction of $CeFe_2$ with H_2. Exposure to hydrogen (≤50 bar) had no effect on $CeFe_2$ at temperatures below 150°C. Figure 8 illustrates the sequence of events which occurred when the alloy was heated in 50 bar H_2 to temperatures in excess of 150°C. At intermediate temperatures new diffraction features can be seen at $2\theta \sim$ 27.5, 28.3, 39.8, and 48.9°. It is likely that these are due to formation of an intermetallic hydride, as no features due to metallic Fe are present; it has not yet been possible to assign a structure to this phase. In addition to these "intermetallic hydride" peaks, features due to the starting material are also visible in diffraction patterns taken at 200°C. Heating to 250°C extinguished these $CeFe_2$ features, and at 300°C the "intermetallic hydride" decomposed into the binary rare earth hydride and iron crystallites. Other authors have observed the same transformation at a similar temperature (*14*).

The sharp Fe peak is a striking feature of the diffraction patterns taken at temperatures above 300°C. This is in marked contrast to the corresponding peak profiles due to both Co and Ru crystallites and corresponds to a particle diameter of ~130 Å; the peak sharpens up slightly on holding the temperature at 450°C (~140 Å crystallites). Growth of the CeH_{2+x} particles also occurred, the size increasing from 85 to 95 Å over a 12-hr period at 450°C. These cerium hydride crystallites were larger than those observed in both $CeRu_2$- and $CeCo_2$-derived catalysts.

b. Interaction of $CeFe_2$ with N_2/H_2. The behavior of $CeFe_2$ in the N_2/H_2 mixture was very different from that in pure hydrogen. Figure 9 shows that exposure of the starting alloy to 50 bar of N_2/H_2 at 450°C produced

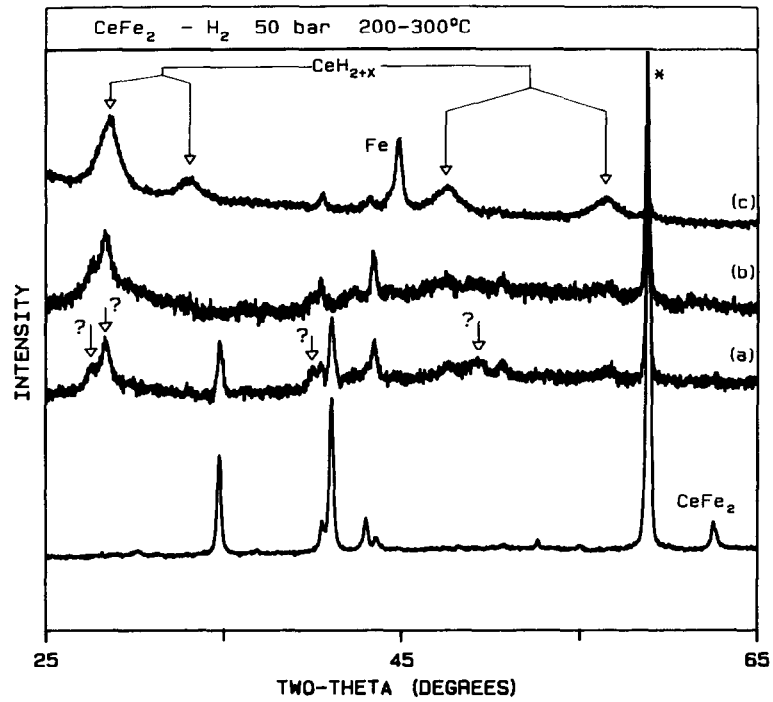

FIG. 8. Hydrogen activation of the $CeFe_2$ precursor alloy at a range of temperatures. (a) 200°C, showing the intermetallic hydride peaks (?); (b) 250°C; (c) 300°C, showing the formation of large iron crystallites.

CeN, as well as CeH_{2+x} and Fe crystallites. However, over a period of 6 hr the CeN peak became less sharp and finally disappeared. During this interval the Fe crystallites increased in size from ~130 to ~140 Å. The CeH_{2+x}/CeN/Fe system exhibited lower activity for ammonia synthesis than both the CeH_{2+x}/Ru and the CeH_{2+x}/CeN/Co catalysts as shown in Table 2. Furthermore, the activity did not correlate at all with the intensity of the CeN peak.

As in the case of one of the $CeRu_2$ precursors, one $CeFe_2$ sample was relatively slow to activate, and in this instance it was again possible to follow the time evolution of the system in more detail. It was found that the onset of ammonia activity *did* coincide with the appearance of CeH_{2+x} and Fe diffraction peaks; furthermore, the increase and leveling-off of the reaction rate paralleled the growth in the number of these crystallites, as was observed for the $CeRu_2$-derived catalyst described earlier. Once again, the ultimate activity of the slow-to-activate sample was the same as that observed with $CeFe_2$ precursors which underwent rapid activation. For this particular $CeFe_2$ sample a very substantial increase in Fe particle size occurred over a 6-hr period (from ~80 to ~130 Å). Furthermore, while the reaction rate did correlate well with the *intensity* of the Fe peak, *there was no correlation between the rate and the exposed surface area of the Fe crystallites as measured by XRD:* this is an observation which is even more striking than that made with the corresponding $CeRu_2$ sample.

c. Interaction of $CeFe_2$ with CO/H_2. $CeFe_2$ did not react with 40 bar of the CO/H_2 mixture at temperatures below 250°C. At this temperature diffraction features characteristic of CeO_2 began to appear, growing in intensity as the temperature was raised to 450°C (Fig. 10); it can be seen that

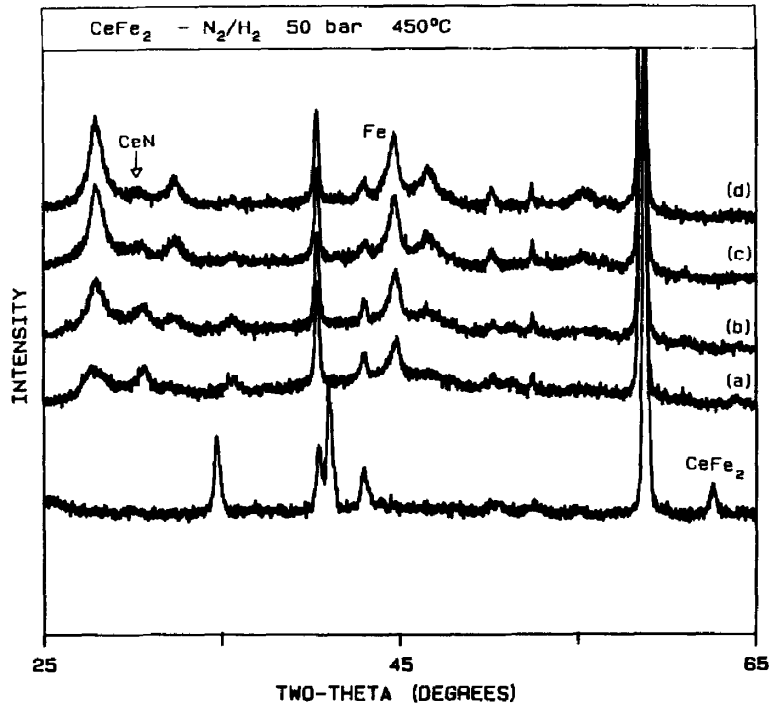

FIG. 9. High-temperature (450°C) N_2/H_2 activation of $CeFe_2$, showing the gradual loss of CeN over a period of time. (a) 1 hr; (b) 2 hr; (c) 4 hr; (d) 6 hr.

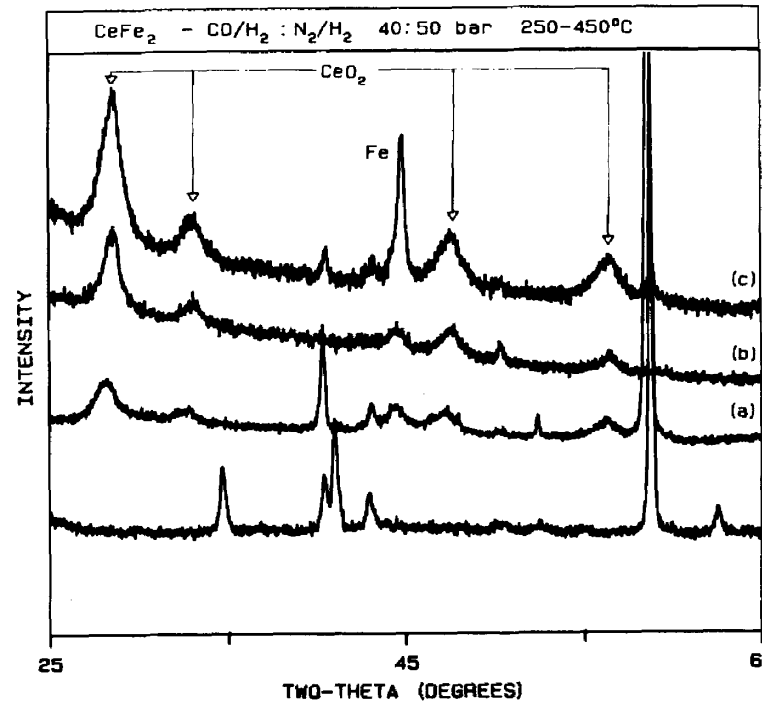

FIG. 10. CO/H_2 preactivation of $CeFe_2$, followed by N_2/H_2 activation. (a) After 1 hr in 40 bar CO/H_2 at 250°C; (b) after 1 hr in 40 bar CO/H_2 at 450°C; (c) after 1 hr in 50 bar N_2/H_2 at 450°C, showing the large increase in intensity and extreme sharpening of the Fe peak which occurs as a result of the $CO/H_2 \rightarrow N_2/H_2$ switch.

under these conditions the Fe peak is small and broad. When the gas feed was switched to 50 bar N_2/H_2 at the same temperature, the Fe peak both increased in intensity and sharpened up considerably. This corresponds to a large increase in the number of crystallites contributing to the Fe peak, as well as a large increase in the size of these crystallites from ~90 to ~180 Å. Further experiments, in which the preactivation time in the CO/H_2 gas feed was varied, showed that this is indeed a real effect, since in every case the peak profile changed dramatically on switching to the N_2/H_2 gas feed. Thus, both the size and the number of Fe crystallites are dependent on the gas feed composition. The CeO_2 crystallite size remained at ~90 Å throughout, approximately the same as that of the CeH_{2+x} particles formed from the $CeFe_2$ precursor. No conversion of CeO_2 to CeN was detectable under ammonia synthesis conditions.

Once again, conversion of the initial intermetallic to rare earth oxide and transition metal particles produced a system which was inactive for ammonia synthesis at 450°C. As with the $CeCo_2$-derived catalyst, raising the temperature to 550°C under 50 bar of the N_2/H_2 mixture did not lead to the onset of detectable ammonia activity. Nor was an active catalyst produced by hydrogenation either at low temperature (to produce the intermetallic hydride) or at high temperature (yielding the binary rare earth hydride) prior to conversion to the oxide. It is also noteworthy that high-temperature (450°C) hydrogenation resulted in the formation of CeH_{2+x} and *large* Fe particles (~130 Å), evidenced by a sharp diffraction peak; this peak did *not* broaden on subsequently switching the gas feed to the CO/H_2 mixture at 450°C but if anything it became sharper.

DISCUSSION

Interaction of hydrogen with RE-transition metal compounds leads to the formation of products which are strongly dependent on the treatment temperature. In general, at low temperatures, an intermetallic hydride which is isostructural with the parent alloy is formed; the associated lattice volume expansion may be as high as 30% (*15*). Hydrogen atoms in these intermetallic hydrides occupy interstitial sites within the metal matrix; hence the hydrides are formed with minimal disruption of the original lattice. This has the consequence that diffraction lines due to the intermetallic hydrides are narrower than those due to the binary rare earth hydride phase, whose formation involves considerable lattice disruption.

Low-temperature interaction of $CeCo_2$ with hydrogen led to an amorphous product whose formation may be rationalized by considering the metastable nature of the intermetallic hydride phase which is likely to precede it. Thus if hydrogenation of the starting alloy were not too vigorous, the temperature would not reach a value high enough to permit significant diffusion of metal atoms. In such a case gross disruption of the metal lattice would not occur and an essentially crystalline intermetallic hydride product might be expected. The observations of Semenenko *et al.* (*14*) are in accord with this. On the other hand if the reaction conditions and exothermicity were to lead to a significant temperature rise, metal diffusion *could* occur. Particle growth would be inhibited by the transient nature of this temperature rise, resulting in the precipitation of X-ray amorphous particles of the decomposition products (binary rare earth hydride and transition metal). Subsequent heating would lead to the growth of X-ray visible crystallites of CeH_{2+x} and metallic Co, as observed experimentally.

Analysis of the products of high-temperature hydrogenation is much more straightforward, since in each case complete hydrogenolysis was observed, yielding crystallites of cerium hydride and transition metal. The observation that the $CeRu_2$-derived intermetallic hydrides are stable to temperatures exceeding those at

which the binary rare earth hydride is preferentially formed indicates that a direct route of alloy hydrogenolysis must exist (i.e., not involving the intermetallic hydride). In passing, it is worth noting that the transition metal particles which were produced are very small (especially in the case of Ru) given the very high transition metal content of these materials. In order to obtain Ru particle sizes of 30–40 Å by conventional techniques, the maximum permissible ruthenium loading would be around 5–7% (*16, 17*).

Interaction of the intermetallic compounds with N_2/H_2 generally followed the trends observed in H_2 alone. However, an additional feature appeared in the diffraction patterns of the $CeCo_2$- and $CeFe_2$-derived systems, which can be attributed to the formation of crystalline cerium nitride; the amount of this phase increased to a constant level in the case of $CeCo_2$, but it gradually decreased to an undetectable level in the iron catalyst. The latter observation may be rationalized in terms of increasing disorder, since the peak broadened significantly before disappearing; why this should happen in one case and not in the other is not clear. The observed formation of CeN is relevant to an earlier report by Takeshita *et al.* (*1*) who stated that CeN peaks were clearly visible in the XRD pattern exhibited by an air-discharged ammonia catalyst derived from $CeCo_2$, although they did not state whether Ce hydride peaks were also present. Peaks due to CeH_{2+x} *can*, however, be seen in their XRD pattern for the air-discharged catalyst derived from $CeRu_2$, while CeN peaks are absent, in agreement with our observations. From a thermodynamic viewpoint CeN is undoubtedly the most favorable product of the interaction of these intermetallics with N_2/H_2. The formation of cerium hydride, which predominates in all cases, must therefore reflect a kinetic barrier to CeN production, possibly a consequence of the high bond strength of the nitrogen molecule. The other possibility is that CeN is produced in a disordered form or as a thin surface layer, so that its presence remained partially ($CeCo_2$ and $CeFe_2$) or completely ($CeRu_2$) undetected.

The most obvious candidate for the active site in these systems would appear to be the transition metal component, since Ru, Co, and Fe are all known to be active for ammonia synthesis. In the two slow-to-activate samples it was observed that the ammonia yield rose with increasing intensities of the transition metal *and* CeH_{2+x} peaks, indicating that creation of one, or both, of these phases gives rise to catalytic activity. Since CeH_{2+x} is known not to be active for the synthesis, it seems likely that transition metal entities constitute the active sites, especially in view of the different activation energies observed for the three CeH_{2+x}/transition metal systems (see Table 2). However, the very different behavior of the CeH_{2+x}- and CeO_2-based systems makes it clear that the role of the support is crucial; this is discussed in more detail below. The activity data clearly demonstrate that CeH_{2+x}/transition metal catalysts are far more active for ammonia synthesis than are the corresponding CeO_2/transition metal systems. The possible role of site-blocking effects due to carbon deposition in the latter case has already been considered and discounted. Encapsulation of the metal phase by CeO_2 appears unlikely in view of the finding that Cu/CeO_2 catalysts produced by these means exhibit exceptionally high methanol synthesis activity (*3*). An-

TABLE 2

Apparent Activation Energies for Ammonia Synthesis[a]

Catalyst precursor	Active system	E_{act}(app.) (kJ/mol)
$CeRu_2$	CeH_{2+x}/Ru	48.5
$CeCo_2$	CeH_{2+x}/Co	33.0
$CeFe_2$	CeH_{2+x}/Fe	42.0

[a] In a 1 : 3 N_2 : H_2 mixture at 50 bar total pressure.

other possibility is that hydrogen spillover from the support to the transition metal crystallites is important, thus rendering CeO_2 relatively ineffectual. Atomic hydrogen *is* certainly present within the cerium hydride support, so the proposal merits further consideration.

CeH_2 adopts the fluorite structure, with hydrogen atoms occupying predominantly the tetrahedral interstices of the fcc metal sublattice. Incorporation of further hydrogen results in filling of the octahedral interstices (*18*). Cerium hydrides, CeH_{2+x} ($x > 0$), dehydrogenate in two steps: hydrogen in the octahedral interstices is liberated at 420°C, followed by hydrogen from the tetrahedral interstices at 850°C (*19*). The relatively low removal temperature of octahedrally coordinated hydrogen strongly suggests that this hydrogen is mobile within the hydride lattice at temperatures relevant to ammonia synthesis. Spillover of atomic hydrogen at the hydride/transition metal interface therefore seems possible. Support for this view comes from the work of Khodakhov *et al.* (*20*) who observed that the catalytic activity of cerium hydride for the hydrogenation of ethylene was associated with the presence of superstoichiometric hydrogen, the stoichiometric compound (CeH_2) being itself inactive. This constitutes clear evidence that weakly held hydrogen in the octahedral interstices may, in certain circumstances, be catalytically active. The spillover hypothesis is further supported by the observation that very slow uptake of hydrogen by metallic Pd at room temperature is greatly accelerated by even *mechanical* contact with cerium hydride (*21*). Phase diagrams indicate that the stoichiometry of the hydride under the conditions employed in this work for ammonia synthesis would lie between $CeH_{2.6}$ (at 400°C) and $CeH_{2.4}$ (at 550°C) (*22*). Mobile hydrogen would thus appear to be plentifully available for spillover.

An alternative interpretation of the large difference in activity observed between hydride and oxide supports comes from a consideration of the mechanism of ammonia synthesis. The rate-determining step is believed to be the dissociation of the nitrogen molecule, with the atomic nitrogen undergoing subsequent hydrogenation on the metal surface (*23, 24*). Furthermore, the production of highly active conventional ammonia catalysts depends critically on the presence of alkali (*25*). This may be rationalized in terms of electron donation from the alkali metal species to the active catalytic site thereby facilitating the dissociative chemisorption of N_2 (*26*). Such a view is supported by the work of Aika *et al.* (*27*) which showed that the rate of ammonia synthesis over promoted ruthenium increased as the ionization potential of the added alkali metal decreased (i.e., Ru–Cs > Ru–K > Ru–Na). Their work also suggested that the support (alumina or active carbon) could act as a medium of electron transfer from alkali to transition metal, implying that direct contact between the promoting species and the active site is not essential for charge transfer to occur.

Another possible explanation can be advanced in terms of SMSI effects. Thus the ammonia synthesis activity of ruthenium on MgO, Al_2O_3, and SiO_2 has been shown (*28*) to follow the sequence

$$MgO \gg Al_2O_3 > SiO_2.$$

EXAFS data (*29*) indicate that with both alumina and silica, a metal–support interaction occurs via oxygen ions of the support; this is consistent with XPS results (*28*) which show that substantial charge transfer occurs from the metal phase. Hence both metallic Ru *and a species interacting with the support* ($Ru^{\delta+}$) are believed to be present in these systems. The lower activity of these catalysts may then be attributed to the presence of these $Ru^{\delta+}$ species, which inhibit nitrogen activation. Under the strongly reducing conditions of ammonia synthesis, however, ruthenium is present purely in its metallic form on MgO, which could account for the far higher ac-

tivity exhibited by this system. In the present case it is therefore possible that the transition metal particles interact with oxygen ions of the CeO_2 support, leading to a depletion of transition metal electron density and correspondingly low ammonia activity. In contrast, the transition metal particles in the CeH_{2+x}/transition metal systems are likely to undergo charge transfer *from* the support, given the electropositive nature of the rare earth hydride (*30, 31*). Enhanced ammonia activity could then result from this interaction. Support for this general view comes from the work of Aika *et al.* (*32*), who report that the turnover frequency of ammonia synthesis over supported Ru is far greater in the Ru/MgO and Ru/CaO systems than it is for the Ru/Al_2O_3 system. They attribute this to differences in electronegativity of the oxide support. This hypothesis is lent further credence by the results of XPS experiments, where the Ru 3*d* binding energy was found to be higher in the Ru/Al_2O_3 case than in both the Ru/MgO and Ru/CaO systems.

The activity loss of CeH_{2+x}/Ru catalysts exposed to air at room temperature for short periods of time cannot be entirely due to the observed hydride → oxide conversion. If such were the case, air-exposed hydride catalysts should exhibit measurable activity at 550°C, and they do not. A possible explanation is that air exposure leads to the formation of Ru in an (amorphous) oxidized, and therefore inactive, form.

The ordering of ammonia activities exhibited by the three systems is of interest: activation in N_2/H_2 produced the sequence $CeRu_2 > CeCo_2 > CeFe_2$. Activation in CO/H_2 also resulted in the $CeRu_2$-derived catalyst exhibiting the highest activity; in this case, the ammonia yield from both the $CeCo_2$- and $CeFe_2$-derived systems was below the detection limit of the apparatus. This ordering contrasts with that reported for the metals themselves which exhibit the sequence Fe > Ru ≫ Co (*33, 34*). Our findings are in agreement with the conclusions of Takeshita *et al.* (*1*), who worked with similar materials and used BET surface areas to arrive at the ordering Ru > Co > Fe.

Nevertheless, it seems reasonable to attribute the ammonia activity of these systems to the transition metal component, since neither cerium oxide nor cerium hydride is known to catalyze the reaction. If the "conventional" sequence (Fe > Ru ≫ Co) is taken as an index of the intrinsic activity of the three metals, three possible explanations for the sequence observed here (Ru > Co > Fe) may be considered:

(a) metal–support interactions affect the three transition metals to different extents,

(b) hydrogen spillover effects from the hydride support occur to different extents,

(c) the particles observed in the diffraction patterns are *not* responsible for the activity of these systems; very small crystallites, invisible to XRD, are in fact the active sites.

These ideas are explored below:

(a) It is well known (e.g., Ref. (*27*)) that ammonia synthesis over Ru catalysts is very sensitive to the presence of promoters. Furthermore, the work of Ozaki *et al.* (*35*) has shown that the activity of K-promoted carbon-supported ammonia catalysts follows the sequence Ru > Co > Fe. It is therefore possible that in the present case, the sensitivity of the transition metal ammonia activity to the promoting action of the hydride support follows the same sequence (Ru > Co > Fe).

(b) If hydrogen spillover effects are important (as suggested by the very different properties of oxide- and hydride-supported catalysts) then the most active sites will presumably be those at the metal–support interface. The greatest number of such sites should occur in the Ru system (followed by Co, then by Fe) in view of the observed average particle sizes.

(c) The final possibility is that crystallites visible by XRD may *not* actually be responsible for the catalytic activity. This hypothesis is consistent with the fact that ammonia activity does not appear to correlate

with transition metal particle size or with any available estimate of exposed metal area. Indeed, earlier work on highly active methanol synthesis catalysts derived from Cu/rare earth alloys has shown that XRD-visible Cu particles are *not* responsible for the observed activity (*3*): it seemed likely that very small Cu entities played the crucial catalytic role. In the present case, this would imply that $CeRu_2$ was the most effective precursor for generating very small transition metal particles. Such an interpretation would be in line with the observed relative sizes of the XRD-visible metal particles (Ru < Co < Fe) and with the higher sintering resistance of Ru (*36*).

A definitive conclusion about these possibilities awaits further structural and mechanistic work on these interesting materials. It seems clear that the high activity is associated in some way with very high dispersion of the transition metal component. However, it is also apparent that some other factor is at work: the difference between oxide- and hydride-supported catalysts points to the operation of some kind of specific metal–support interaction, possibly involving the spillover of hydride hydrogen. Work is under way in our laboratory which is aimed at addressing some of these issues.

CONCLUSIONS

1. Decomposition of $CeRu_2$, $CeCo_2$, and $CeFe_2$ intermetallic alloys in N_2/H_2 produces CeH_{2+x}/transition metal systems which are active and thermally stable ammonia synthesis catalysts.

2. Although cerium nitride was formed during activation of $CeCo_2$ and $CeFe_2$ precursors, this phase plays no role in the ultimate catalytic activity.

3. Prior formation of intermetallic hydrides has no effect upon the activity for the systems studied.

4. For catalysts which activated slowly, there was good correlation between the rising rate of ammonia synthesis and the growth of both cerium hydride and the transition metal crystallites; this suggests that the active site is associated with the creation of one or possibly both of these phases.

5. The corresponding CeO_2/transition metal systems produced by reaction with CO/H_2 were catalytically almost inert, despite having metal dispersions comparable with those of the CeH_{2+x}-based materials. Likewise, oxidation of the hydride-based catalysts to yield CeO_2 led to a large and irreversible loss of activity.

6. Although most of the transition metal in these catalysts is visible by XRD, in every case there was no correlation between the surface area estimated by XRD and the catalytic activity of the system.

7. The special activity of these catalysts seems to derive from an intimate interaction between the cerium hydride "support" and the transition metal component; the latter may be present in a highly dispersed form.

ACKNOWLEDGMENTS

This work was supported by SERC/CASE Award 86CD044 (APW) in collaboration with ICI plc and by the provision of equipment under SERC Grant GRD 25019. We are indebted to Dr. G. Owen for preparing the intermetallic compounds and we thank Dr. R. M. Nix for helpful and stimulating discussions.

REFERENCES

1. Takeshita, T., Wallace, W. E., and Craig, R. S., *J. Catal.* **44,** 236 (1976).
2. Baglin, E. G., Atkinson, G. B., and Nicks, L. J., *Ind. Eng. Chem. Prod. Res. Dev.* **20,** 87 (1981).
3. Nix, R. M., Rayment, T., Lambert, R. M., Jennings, J. R., and Owen, G., *J. Catal.* **106,** 216 (1987).
4. Compton, V. B., and Matthias, B. T., *Acta Crystallogr.* **12,** 651 (1959).
5. Van Essen, R. H., and Buschow, K. H. J., *J. Less-Common Met.* **70,** 189 (1980).
6. Buschow, K. H. J., and van Wieringen, S. J., *Phys. Status Solidi* **42,** 231 (1970).
7. Tessema, G. X., Peyrard, J., Nemoz, A., Senateur, J. P., Rouault, A., and Fruchart, R., *Z. Phys. Chem. Neue Folge* **116,** S209 (1979).
8. Fruchart, D., Vaillant, F., Roudaut, E., Nemoz, A., and Tessema, X. G., *Phys. Status Solidi (a)* **65,** K19 (1981).

9. Fruchart, D., Vaillant, F., Rouault, A., Benout, A., and Flouquet, J., *J. Less-Common Met.* **101,** 285 (1984).
10. Libowitz, G. G., and Maeland, A. J., *in* "Handbook on the Physics and Chemistry of the Rare Earths" (K. A. Gschneider, Jr., and L. Eyring, Eds.), Vol. 3, p. 303. North-Holland, Amsterdam, 1979.
11. Rienäcker, G., and Birckenstaedt, M., *Z. Anorg. Allg. Chem.* **265,** 99 (1951).
12. Shedd, E. S., and Henrie, T. A., "Proceedings, Conf. Rare Earth Res., 3rd, Clearwater, FL," p. 21, 1963.
13. Mills, G. A., and Steffgen, F. W., *Catal. Rev. Sci. Eng.* **8,** 159 (1974).
14. Semenenko, K. N., and Burnasheva, V. V., *J. Less-Common Met.* **105,** 1 (1985).
15. Yartys, V. A., Burnasheva, V. V., Semenenko, K. N., Fadeeva, N. V., and Solov'ev, S. P., *Int. J. Hydrogen Energy* **7,** 957 (1982).
16. Dalla Betta, R. A., *J. Catal.* **34,** 57 (1974).
17. Gay, I. D., *J. Catal.* **80,** 231 (1983).
18. Holley, C. E., Mulford, R. N. R., Ellinger, F. H., Koehler, W. C., and Zachariasen, W. H., *J. Phys. Chem.* **59,** 1226 (1955).
19. Dmitrieva, V. N., Rezukhina, T. N., Varekha, L. M., Vorob'ev, V. D., Domashev, V., F., Gusynin, B. A., Kravchenko, L. I., and Mel'nikova, V. A., *Metallofizika* **49,** 109 (1973).
20. Khodakhov, Yu. S., Torbin, S. N., and Minachev, Kh. M., *Izv. Akad. Nauk. SSSR Ser. Khim.* **5,** 1048 (1972).
21. Wicke, E., Küssner, A., and Otto, K., "Actes Intern. Congr. Catalyse, 2e, Paris, 1960," p. 1035. Editions Technip, Paris, 1961.
22. Hardcastle, K. I., and Warf, J. C., *Inorg. Chem.* **5,** 1728 (1966).
23. Bokhoven, C., Gorgels, M. J., and Mars, P., *Trans. Faraday Soc.* **55,** 315 (1959).
24. Yamamoto, O., Tanaka, S., and Tanaka, K., *Sci. Pap. Int. Phys. Chem. Res.* **68,** 8 (1974).
25. Mittasch, A., "Advances in Catalysis," Vol. 2, p. 81. Academic Press, New York, 1950.
26. Jenikjev, E. K., and Krylova, A. V., *Kinet. Catal. (Eng. Ed.)* **3,** 16 (1962).
27. Aika, K. I., Hori, H., and Ozaki, A., *J. Catal.* **27,** 424 (1972).
28. Bossi, A., Garbassi, F., and Petrini, G., *J. Chem. Soc. Faraday Trans. 1* **78,** 1029 (1982).
29. Lytle, F. W., Via, G. H., and Sinfelt, J. H., *J. Chem. Phys.* **67,** 3831 (1977).
30. Ward, J. W., *J. Less-Common Met.* **73,** 183 (1980).
31. Switendick, A. C., *Top. Apply. Phys.* **28,** 101 (1978).
32. Aika, K. I., Ohya, A., Ozaki, A., Inoue, Y., and Yasumori, I., *J. Catal.* **92,** 305 (1985).
33. Rambeau, G., and Amariglio, H., *J. Catal.* **72,** 1 (1981).
34. Rambeau, G., Jorti, A., and Amariglio, H., *J. Catal.* **94,** 155 (1985).
35. Ozaki, A., Aika, K. I., and Hori, H., *Bull. Chem. Soc. Japan* **44,** 3216 (1971).
36. Wanke, S., and Flynn, P. C., *Catal. Rev. Sci. Eng.* **12,** 93 (1975).